

## MIT Open Access Articles

*Reactivity of Crystalline Slags in Alkaline Solution*

The MIT Faculty has made this article openly available. **Please share** how this access benefits you. Your story matters.

**As Published:** 10.1007/978-3-030-10386-6\_21

**Publisher:** Springer International Publishing

**Persistent URL:** <https://hdl.handle.net/1721.1/136030>

**Version:** Author's final manuscript: final author's manuscript post peer review, without publisher's formatting or copy editing

**Terms of use:** Creative Commons Attribution-Noncommercial-Share Alike



# Reactivity of crystalline slags in alkaline solution

Brian Traynor<sup>a</sup>, Hugo Uvegi<sup>a</sup>, Piyush Chaunsali<sup>b</sup>, Elsa Olivetti<sup>a\*</sup>

<sup>a</sup> Department of Materials Science and Engineering, MIT, Cambridge, USA

<sup>b</sup> Department of Civil Engineering, IIT Madras, Chennai, India

\* Corresponding author: [elsao@mit.edu](mailto:elsao@mit.edu)

Keywords: Slag, Alkali Activation,  $\gamma$ -C<sub>2</sub>S

## 1. Abstract

Slags with varied amorphous and crystalline content, typical of iron and steel production, are generally under-utilized. One promising re-use pathway for these wastes is chemical activation, producing alternatives to conventional building materials with lower embodied energy. The formation of a hardened binder is dependent on the slag mineralogy and, specifically, the reactivity of relevant phases. Reactivity can be understood by monitoring elemental dissolution rates through inductively couple plasma (ICP-OES) analysis. Post-dissolution ICP analysis of activating solution and spectroscopic analysis of remaining solids was performed on several highly crystalline slags and on relevant synthetic minerals to track changes in chemical and phase composition. Amorphous and ionic phases have been observed as more reactive than other crystalline phases. This work aims to inform future studies on waste blending in alkali activated systems, a promising avenue for valorization of industrial wastes with varied physico-chemical properties. To this end, dissolution tests with varied initial Si, Al, and Ca concentrations in activating solution were also performed.

## 2. Introduction

Concerns over the CO<sub>2</sub> emissions associated with the cement industry have led to greater research efforts being devoted to the development of alternative, lower energy-embodied binders. One such family of alternative binders is alkali activated materials. Alkali activated materials use precursors rich in silica and alumina with variable amounts of calcium in an aqueous alkaline environment to form hardened aluminosilicate networks with comparable physical properties to Portland cement-based binders. While traditional cements are hydraulic in nature, relying on the reaction of calcium silicates in the presence of water to form calcium silicate hydrate, alkali activated materials require an alkali activating solution to promote the reaction of an aluminosilicate source to form a hardened material. One of the strengths of alkali activated materials is the versatility in potential precursors. One high-volume source of potential precursors is industrial byproducts from the metals and energy generation industries. Beneficiation of industrial wastes in alkali activated materials can provide a construction material with lower environmental impact than conventional construction materials [1]. For example, a great deal of research has been devoted to development of binders based on blast furnace slag and fly ash activated by an alkali activator, typically sodium hydroxide or sodium silicate [2, 3].

However, any attempt to reduce the environmental effect of the production of conventional construction materials cannot rely on these materials (blast furnace slag and fly ash) alone. Expansion of the range of suitable precursors to other industrial byproducts represents an opportunity to develop a more adaptable pool of precursors for construction materials in which locally available wastes can substitute for existing construction materials. Mismatches between local supply of suitable wastes and demand for construction materials requires a more flexible toolkit of load-bearing materials based on industrial byproducts. One strategy to negate this problem is to design a load-bearing material, in which the shortcomings in a locally available precursor may be overcome through chemical activation (alkali activation) and/or by blending with another precursor. In terms of material chemistry, highly siliceous precursors can be blended with calcium rich precursors in appropriate ratios to synthesize a calcium silicate hydrate phase, for example [4]. Blending of materials is particularly pertinent in the case of poorly reactive wastes or wastes with high variability in their composition or physical properties. One family of underutilized wastes are crystalline slags.

Crystalline slag is a byproduct of the steel, iron and copper industries. Crystalline slags are produced when slags are air-cooled upon tapping from the blast furnace. A poorly cementitious material, crystalline slag is used in low-value applications, such as land reclamation and aggregate in construction materials. However, slags of this kind are rich in silica, alumina, and calcia – chemical constituents that form reaction products that provide strength to a load-bearing material. Globally, an estimated 220 million metric tons of steel slag and an estimated 25 million metric tons of copper slag were produced in 2016 [5, 6].

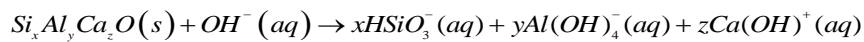
The reaction pathway for strength-giving phases in a construction material take place in aqueous phase. Precursors release chemical species under the influence of an activator and organize in solution to form a reaction product that binds the structure together, endowing the material with strength. This study examines the dissolution kinetics of crystalline phases commonly found in crystalline slags with the goal of improving our understanding of how blending crystalline slags with other materials will impact the rate of dissolution.

### 3. Background

#### 3.1 Thermodynamic basis

Substituting for existing high embodied energy construction materials with slags requires an understanding of the properties of the constituent crystal phases of the slag. The dissolution of crystal phases in solution is dependent on many factors, including temperature, activities of dissolved species, ionic strength of dissolving solution, surface area of dissolving mineral, and surface structure of dissolving mineral. The basis for alkali activation rests on the fact that alkaline environment promotes rapid dissolution of a range of aluminosilicate precursors. In order to expand the pool of potential construction material precursors, the effect of alkali solution on the dissolution of the constituent phases of any potential precursor must be understood.

However, controlling all variables in a dissolution experiment is a fundamental challenge in determining solubility constants and understanding changes in dissolution rate as a function of undersaturation. Controlling for temperature and ionic strength is generally achievable, the latter being achieved by performing dissolution experiments in dilute environment, such that species dissolving from minerals do not appreciably affect the overall ionic strength of the solution, while still being measurable through ICP. Some control over mineral surface area can be achieved through limitations on particle sizes used. However, this parameter can change as a function of time if minerals dissolve rapidly. In this study, the minerals of interest are expected to dissolve slowly, suggesting that it is possible to control for surface area. The other most significant factor in mineral phase dissolution is the activities of the dissolved species. The thermodynamic driving force for dissolution of a mineral phase is the difference in Gibbs energy between the mineral phase and its constituent chemical species in the aqueous phase. For a given calcium aluminosilicate phase, the (unbalanced) dissolution reaction in basic medium may proceed as;



This reaction will proceed to the right until equilibrium is reached, defined by the Gibbs free energy of the reaction. The Gibbs free energy of this reaction is given by;

$$\Delta G_{rxn} = \Delta G_{rxn}^0 + RT \ln(IAP)$$

where  $\Delta G_{rxn}$  is the Gibbs free energy of the reaction,  $\Delta G_{rxn}^0$  is the Gibbs free energy for the reaction in its standard state, and IAP is the ion activity product of the aqueous species. At equilibrium, the Gibbs free energy of the reaction is zero, and  $IAP = K_{SP}$ . The value  $K_{SP}$  is the ion activity product for the activities at equilibrium. A new quantity, the chemical affinity can then be described, which is a measure of the distance from equilibrium of a reaction, and hence the magnitude of the driving force for the reaction to proceed. The chemical affinity can be written as;

$$A = -RT \ln \left( \frac{IAP}{K_{SP}} \right)$$

Rates of dissolution are a complex function of the chemical affinity. The chemical affinity does not account for surface areas and defects on surfaces, which can influence dissolution kinetics profoundly [7]. However, there generally exists a so-called “dissolution plateau” at very high chemical affinities in which the rate of dissolution is high enough to be independent of surface defects and is constant over a range of ion activities [8]. As the concentration of aqueous species increases over time, other phases are liable to precipitate from solution. Maintaining a highly dilute solution can also prevent the precipitation of these phases.

Through carefully designed experiments, the rate of dissolution of a given crystal phase can be investigated. Additionally, the initial concentration of other elements can be varied to examine the effects of blending of crystalline slags with other materials. The most important elements in this regard are Al, Si, and Ca. Concentrations of these elements in solution model the effects of simultaneous dissolution of other cementitious and pozzolanic materials, such as Portland cement, fly ash, biomass ash, blast furnace slag, and hydrated lime. The presence of these elements may change the ion activity product of the solution, changing the chemical

affinity for dissolution of the mineral of interest. However, in highly dilute systems, the more likely effect is on the rate of dissolution is expected to come from inhibition or catalysis of dissolution of the mineral phase by aqueous Al, Si, or Ca. For example, the mechanism of aluminosilicate glasses is known to be inhibited by the presence of aqueous Al [9]. Experiments such as these take a macroscopic approach to understanding the mechanism of material dissolution through analysis of dissolution data.

### 3.2 $\gamma$ -C<sub>2</sub>S

Gamma dicalcium silicate ( $\gamma$ -C<sub>2</sub>S) is a crystalline phase commonly found in steel slags and is identified as an understudied abundant mineral phase. Dicalcium silicate has five main polymorphs;  $\alpha$ ,  $\alpha'$ ,  $\alpha'_H$ ,  $\beta$ , and  $\gamma$ . The  $\gamma$  polymorph is the only phase stable at room temperature, forming below 500°C. The  $\beta$  polymorph when stabilized in the presence of other impurities is known as belite in cement chemistry and reacts rapidly with water. Studies have assessed the cementitious properties of  $\gamma$ -C<sub>2</sub>S and concluded that is generally non-hydraulic phase [10, 11, 12]. Other work has sought to develop ways in which  $\gamma$ -C<sub>2</sub>S can be hydrated, both by means of chemical activation and mechanical activation [13, 14]. However, little work has been done to determine the solubility constant, the relationship between undersaturation and dissolution rate, or the effect of aqueous species on the mechanism of dissolution. Additionally, little work has been done to explore the effects of blending of  $\gamma$ -C<sub>2</sub>S containing materials with other, more reactive phases. This study investigates the effects of undersaturation and aqueous concentration of Al, Si, and Ca on dissolution rate in sodium hydroxide solution to lay the groundwork for exploration of blending of  $\gamma$ -C<sub>2</sub>S bearing slags with other materials.

## 4. Experimental Procedures

### 4.1 Materials

Three crystalline slags were used in this study. Two slags were sourced from Haryana, India. These slags are identified as Bansal slag and DA slag. Both slags are cupola slags, a byproduct of pig iron production in so called “cupola furnaces”. The third slag is a steel ladle slag sourced from the US (Arcelor Mittal), identified as “Ladle slag”. Ladle slag is a byproduct of steel refinement following production of steel from a basic oxygen furnace or electric arc furnace.

$\gamma$ -C<sub>2</sub>S can be synthesized via a modified Pechini synthesis or sintering of precursor oxides. Olav et al [15] defines the modified Pechini process for the synthesis of oxides as starting with a homogeneous aqueous solution containing the desired cation precursors in stoichiometric ratio and selected additives, which by evaporation and reactions is converted to a rigid cross linked polymer hindering segregation of cation. The polymer is further converted to a homogenous powder by heat treatment. Nettleship et al used this process to synthesize high purity  $\gamma$ -C<sub>2</sub>S from calcium nitrate and colloidal silica precursors [11]. The additives used to produce the host gel are ethylene glycol and citric acid monohydrate.  $\gamma$ -C<sub>2</sub>S may also be synthesized by sintering of a pellet of the comprised of the constituent oxides or carbonates – silica and calcium carbonate in this case – at high temperatures, as described by Kriskova et al [16].

### 4.2 Mineral content analysis

Identification and quantification of the mineral phases present in slags was achieved through X-ray diffraction and Rietveld analysis. XRD data was collected using high speed Bragg-Brentano optics on a PANalytical X'Pert Pro MPD operated at 45 kV and 40 mA. Data was obtained between 5° and 70° (2 $\theta$ ) using a step size of 0.0167° with each sample scan lasting 52 minutes. The diffractometer was configured with a 1/2° divergent slit, a 0.04 radian soller slit, and a 1° anti-scatter slit. The powdered sample was packed into a 27 mm diameter sample holder. HighScore Plus software was used for quantitative X-ray diffraction.

### 4.3 Dissolution experiments

Dissolution experiments were performed in batch reactors at 20°C; 500mL pre-cleaned HDPE bottles containing 250mL of solution. Containers were cleaned using nitric acid and Millipore water. Solutions were gently agitated initially, but not stirred to prevent particle abrasion. Sodium hydroxide was used as an alkali activator at concentrations of 0.1M and 1M. Sodium hydroxide solutions were prepared using Millipore water (18.2 M $\Omega$ .cm) and analytical grade NaOH. The pH of these solutions was measured before introduction of mineral phase. Solutions with initial concentrations of Al, Si, and Ca were prepared through additions of reagent grade Al(NO<sub>3</sub>)<sub>3</sub>·9H<sub>2</sub>O, Ca(OH)<sub>2</sub> and SiO<sub>2</sub>. Appropriate quantities of the synthetic mineral of interest were added to the batch reactor to initiate dissolution. 5mL aliquots of solution were removed at regular intervals, with the removed volume of solution being replaced by fresh NaOH solution of the appropriate concentration. Aliquots were filtered (<0.2 $\mu$ m) and diluted in 2% nitric acid matrix for ICP-OES analysis on an Agilent 5100 Vertical Dual View ICP-OES. Al, Si, and Ca concentrations were measured directly by ICP-OES analysis at concentrations between 0.1 and 200 mg/L, with the dilution in 2% HNO<sub>3</sub> reflecting this desired concentration. Remnant solids were immersed in isopropyl alcohol to halt hydration before being dried and stored under

nitrogen in a desiccator. Hydroxide ion concentrations were calculated using the extended Debye-Hückel equation [17] and pH measurements taken using an Orion Star A111 pH meter. The pH meter was calibrated against a series of NaOH solutions of known concentrations. The solution-mineral mass ratio was chosen to ensure no precipitation of reaction products, and to measure the rate of dissolution far from equilibrium in the so-called “dissolution plateau”.

#### 4.4 Ion activities

Ion activity products were calculated using Gibbs free energy minimization software, GEM-Selektor v3.3 with PSI-Nagra and CEMDATA18 thermodynamic databases. The activities of charged aqueous species was calculated using the Helgeson form of the (Truesdell-Jones) extended Debye-Hückel equation with ion size parameters and extended term parameters for NaOH [17]. The activity of water was calculated using the osmotic coefficient and the extended term used to calculate the activity coefficients for neutral aqueous species.

## 5. Results

### 5.1 Crystalline slags

#### 5.1.1 Chemical and mineral composition

Chemical composition from X-ray fluorescence (XRF) measurements are shown in Table 1. Bansal and DA slags have similar chemical compositions as a consequence of the similar feedstocks used at both plants. The Ladle slag had relatively high calcia and alumina content. High calcium and aluminum content is typical for ladle slags and thus is expected [18], [19]. The composition of the Bansal and DA slags is typical of slags from pig iron production [20].

	<b>Bansal slag</b>	<b>DA slag</b>	<b>Ladle slag</b>
SiO <sub>2</sub>	50.8	46.49	3.84
Al <sub>2</sub> O <sub>3</sub>	11.3	18.79	28.63
Fe <sub>2</sub> O <sub>3</sub>	10.8	6.11	4.66
CaO	17.7	17.06	51.38
MgO	5	6.15	6.88
Na <sub>2</sub> O	0.01	0.42	0.07
K <sub>2</sub> O	0.5	0.93	0.07
TiO <sub>2</sub>	1.3	1.48	0.14
MnO <sub>2</sub>	2.98	1.96	0.78
P <sub>2</sub> O <sub>5</sub>	0.16	0.15	0.06
SrO	0	0.05	0.03
BaO	0.18	0.12	0.01
SO <sub>3</sub>	0.12	0.29	1.51
LOI	0	0.02	1.94

Table 1 - Chemical composition of crystalline slags as determined by XRF

The XRD patterns of the 3 slags of interest is shown in Figure 1. The phase distribution of these slags is markedly different. Only the major phases are identified in each case. The ladle slag is primarily composed of calcium aluminate phases and periclase. Despite having similar chemical compositions, the Bansal and DA slags have contrasting mineralogy. The Bansal slag is primarily composed of the pyroxene mineral diopside. The closely related mineral hedenbergite and augite are also detected in the Bansal slag due to the substitution of Fe, Na and Ti. In contrast, the DA slag is semi-crystalline and shows the presence of anorthite and quartz as major phases as well as an amorphous phase.

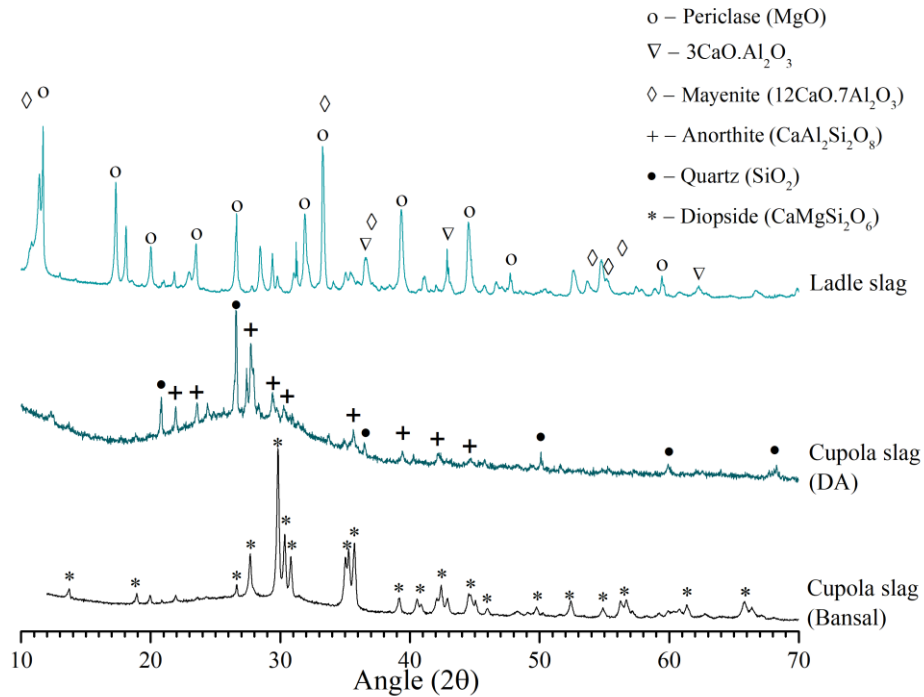


Figure 1 - Phase distribution of crystalline slags. Only major crystalline phases are identified here

### 5.1.2 Dissolution of slags

Each of the slags was exposed to NaOH solutions of 0.1M and 1M for up to 48 hours to assess the reactivity of the slags upon exposure to an alkali activator. The phase distribution of each slag was determined after prolonged dissolution (1 week) to those phases which are reactive in the presence of alkali activator. In the case of the Bansal and DA slag, no major differences in phase distribution were observed and are thus not shown here. However, upon exposure to NaOH solution, calcium aluminate phases of the Ladle slag are observed to be consumed and portlandite is observed to precipitate. Mayenite and C3A (3CaO·Al<sub>2</sub>O<sub>3</sub>) are observed to react rapidly, liberating calcium into solution. The high concentration of OH<sup>-</sup> ions in solution drives formation Ca(OH)<sub>2</sub>.

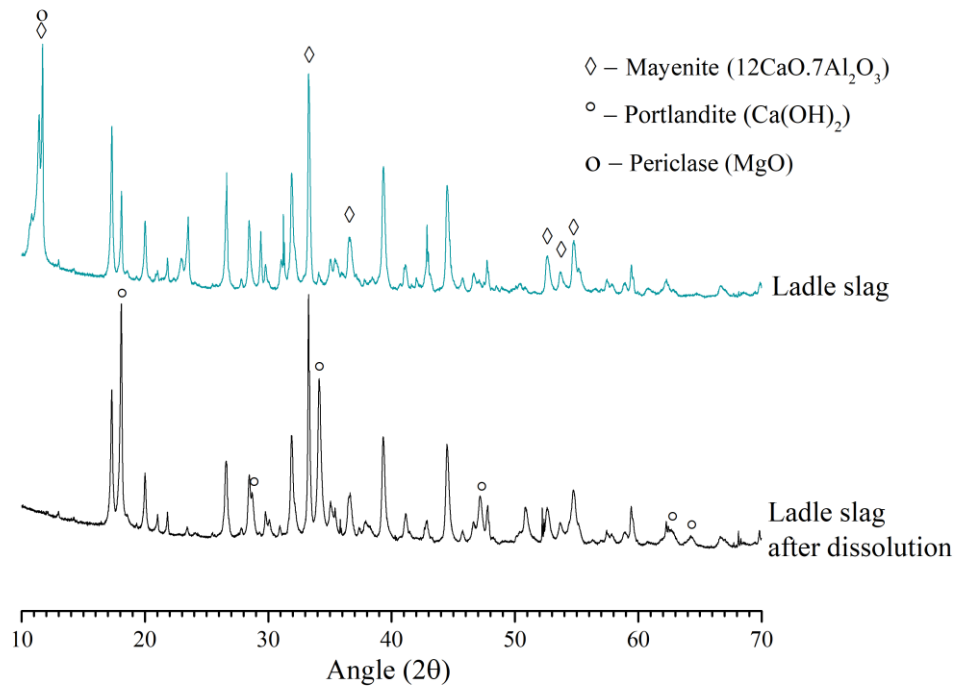


Figure 2 - Change in phase distribution of Ladle slag after exposure to NaOH activating solution

Dissolution of major elements from slags is recorded using ICP-OES analysis, shown in Figure 3 and 4 at NaOH concentrations of 1M ( $\text{pH} \approx 13.6$ ) and 0.1M ( $\text{pH} \approx 13$ ) respectively. Dissolution data for Al, Ca and Si is shown. Dissolution data for Fe, Mg, Na and S were also recorded but negligible concentration of these elements was observed and thus are not included here.

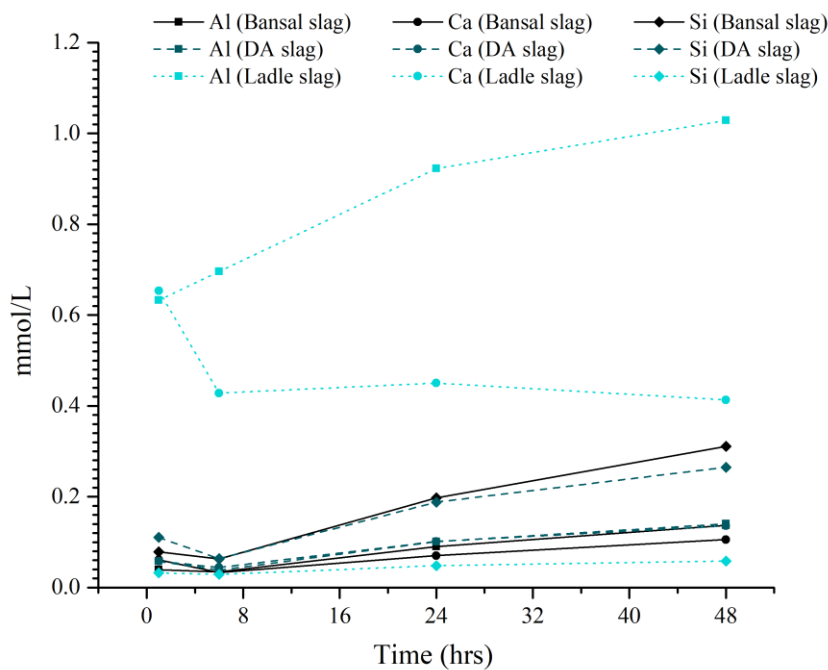


Figure 3 - Dissolution kinetics of Bansal, DA and Ladle slag in 1M NaOH solution at L/S of 1000.

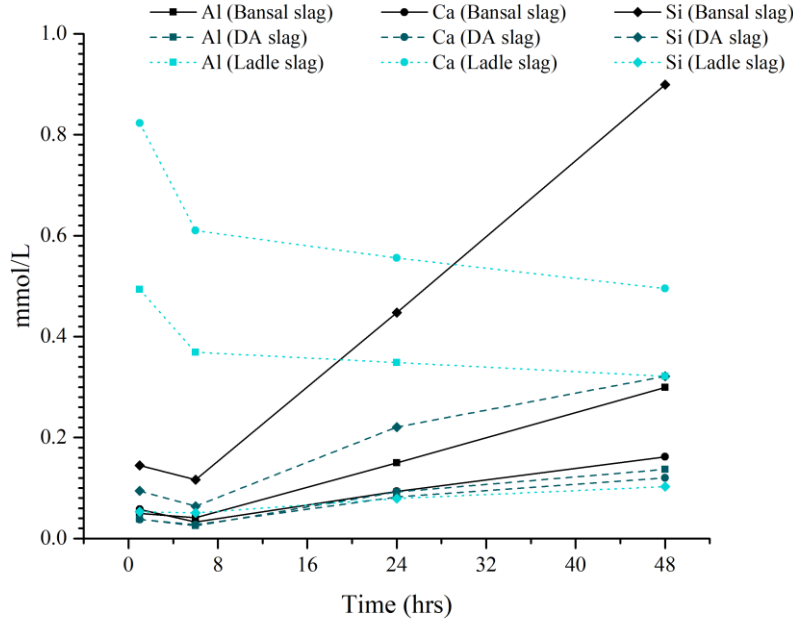


Figure 4 - Dissolution kinetics of Bansal, DA and Ladle slag in 0.1M NaOH solution at L/S of 1000.

After 1 hour, the dissolution Al and Ca from the Ladle slag is approximately 1 order of magnitude larger than concentrations of elements from the other slags. This very high initial concentration is indicative of the presence of highly reactive phases in the Ladle slag, already identified in Figure 2 as being due to C3A and mayenite. The concentration of silicon from the Ladle slag remains low, as expected from the low silicon content of the slag. The evolution of the Al and Ca concentrations over time sees a gradual decrease in concentration in the case of the 1M NaOH solution. This decrease is suggestive of the formation and precipitation of reaction products due to supersaturation of reaction products. In the case of the 0.1M NaOH solution, the Al concentration gradually increases, while the Ca concentration decreases over time. The decrease in Ca concentration is understood to be due to precipitation of  $\text{Ca}(\text{OH})_2$ . The saturation point of Ca in solution is reached at much lower concentrations than the saturation point of Al in basic solution. In the case of the 0.1M NaOH, the  $\text{OH}^-$  concentration is sufficiently low to prevent the formation of  $\text{Al}(\text{OH})_3$ , allowing continued increase of Al concentration in solution.

The Bansal and DA slags demonstrate very similar dissolution kinetics. In all cases, the concentration of Al, Ca and Si increases approximately linearly after 6 hours. The kinetics of dissolution are faster in the more basic 1M NaOH than the 0.1M NaOH for the Bansal and DA slags. The reason for the decrease in concentration from 1 hour to 6 hours is unknown, and further analysis of slag post-dissolution is required. The solubility limit of Al, Ca or Si is not expected to be reached within this time period, nor are reaction products predicted to precipitate.

Despite the presence of an amorphous phase, the kinetics of dissolution of the DA slag are slower than the chemically similar Bansal slag due to differences in mineralogy. While amorphous content is frequently a good indicator of reactivity, it is necessary to build an understanding of the kinetics of dissolution of other mineral phases found in the slag to better understand the potential of crystalline slags in construction materials. A more comprehensive understanding of how the kinetics of dissolution of these phases is influenced by the presence of other chemical species in solution can also provide insight into the potential effects of blending, whereby a more reactive material is mixed with a less reactive one to produce a load-bearing material.

## 6. Acknowledgements

We would like to acknowledge the financial support for this research through the Tata Center for Technology and Design as well as the Environmental Solutions Initiative, both at Massachusetts Institute of Technology (MIT), Cambridge. We also acknowledge support from NSF CAREER #1751925.



## 7. References

- [1] B. C. McLellan, R. P. Williams, J. Lay, A. Van Riessen, and G. D. Corder, “Costs and carbon emissions for geopolymer pastes in comparison to ordinary portland cement,” *J. Clean. Prod.*, vol. 19, no. 9–10, pp. 1080–1090, 2011.
- [2] I. Ismail, S. A. Bernal, J. L. Provis, R. San Nicolas, S. Hamdan, and J. S. J. Van Deventer, “Modification of phase evolution in alkali-activated blast furnace slag by the incorporation of fly ash,” *Cem. Concr. Compos.*, vol. 45, pp. 125–135, 2014.
- [3] P. Duxson and J. L. Provis, “Designing precursors for geopolymer cements,” *J. Am. Ceram. Soc.*, vol. 91, no. 12, pp. 3864–3869, 2008.
- [4] P. Chaunsali *et al.*, “Mineralogical and microstructural characterization of biomass ash binder,” *Cem. Concr. Compos.*, vol. 89, pp. 41–51, 2018.
- [5] H. G. van Oss, “Mineral Commodity Summaries,” 2017.
- [6] M. Brininstool and D. M. Flanagan, “2015 Minerals Yearbook - Copper,” 2015.
- [7] A. Luttge, “Crystal dissolution kinetics and Gibbs free energy,” vol. 150, pp. 248–259, 2006.
- [8] K. L. Nagy and A. C. Lasaga, “Dissolution and precipitation kinetics of gibbsite at 80°C and pH 3: The dependence on solution saturation state,” *Geochim. Cosmochim. Acta*, vol. 56, no. 8, pp. 3093–3111, 1992.
- [9] R. Snellings, “Surface chemistry of calcium aluminosilicate glasses,” *J. Am. Ceram. Soc.*, vol. 98, no. 1, pp. 303–314, 2015.
- [10] S. N. Ghosh, P. B. Rao, A. K. Paul, and K. Raina, “The chemistry of dicalcium silicate mineral,” *J. Mater. Sci.*, vol. 14, pp. 1554–1566, 1979.
- [11] I. Nettlehip, J. L. Shull, and W. M. Kriven, “Chemical Preparation and Phase Stability of Ca<sub>2</sub>SiO<sub>4</sub> and Sr<sub>2</sub>SiO<sub>4</sub> Powders,” *J. Eur. Ceram. Soc.*, vol. 11, pp. 291–298, 1993.
- [12] J. Bensted, “Gamma-dicalcium silicate and its hydraulicity,” *Cem. Concr. Res.*, vol. 8, pp. 73–76, 1978.
- [13] L. Kriskova *et al.*, “Effect of mechanical activation on the hydraulic properties of stainless steel slags,” *Cem. Concr. Res.*, vol. 42, no. 6, pp. 778–788, 2012.
- [14] L. Kriskova *et al.*, “Influence of mechanical and chemical activation on the hydraulic properties of gamma dicalcium silicate,” *Cem. Concr. Res.*, vol. 55, pp. 59–68, 2014.
- [15] T. Olav, L. Sunde, T. Grande, and M. Einarsrud, “Modified Pechini Synthesis of Oxide Powders and Thin Films,” pp. 1–30, 2016.
- [16] L. Kriskova *et al.*, “Hydraulic behavior of mechanically and chemically activated synthetic merwinite,” *J. Am. Ceram. Soc.*, vol. 97, no. 12, pp. 3973–3981, 2014.
- [17] H. C. Helgeson, “Prediction of the thermodynamic properties of electrolytes at high pressures and temperatures,” *Phys. Chem. Earth*, vol. 13–14, pp. 133–177, 1981.
- [18] C. Shi, “Characteristics and cementitious properties of ladle slag fines from steel production,” *Cem. Concr. Res.*, vol. 32, no. 3, pp. 459–462, 2002.
- [19] D. Adolfsson, R. Robinson, F. Engström, and B. Björkman, “Influence of mineralogy on the hydraulic properties of ladle slag,” *Cem. Concr. Res.*, vol. 41, no. 8, pp. 865–871, 2011.
- [20] A. Monshi and M. K. Asgarani, “Producing portland cement from iron and steel slags and limestone,” *Cem. Concr. Res.*, vol. 29, no. 9, pp. 1373–1377, 1999.